2013

Constitutive mu-Opioid Receptor Activity Leads to Long-Term Endogenous Analgesia and Dependence

Gregory Corder, *University of Kentucky*
Suzanne Doolen, *University of Kentucky*
Renee R. Donahue, *University of Kentucky*
Michele K Winter, *University of Kansas Medical Center*
Brandon L Jutras, *University of Kentucky*, et al.

Constitutive μ-Opioid Receptor Activity Leads to Long-Term Endogenous Analgesia and Dependence

G. Corder *et al.*

Science **341**, 1394 (2013);
DOI: 10.1126/science.1239403

of *cGas*$^{-/-}$ mice are strikingly similar to those of *Sting*$^{-/-}$ mice [this study and (*18*)]. These results, together with our biochemical data showing that cGAS is a cytosolic enzyme activated by its binding to generic DNA (*2*, *3*), formally demonstrate that cGAS is a nonredundant and general cytosolic DNA sensor that activates STING.

We present evidence that 2′3′cGAMP is an effective adjuvant that boosts the production of antigen-specific antibodies and T cell responses in mice. Although the bacterial second messengers cyclic di-GMP and cyclic di-AMP are being developed as potential vaccine adjuvants (*22*), 2′3′cGAMP is a much more potent ligand of STING than any of the bacterial cyclic dinucleotides (*7*). Thus, 2′3′cGAMP may be developed as an adjuvant for next-generation vaccines to prevent or treat human diseases, including infectious diseases and cancer.

References and Notes

1. L. A. O'Neill, *Science* **339**, 763–764 (2013).
2. L. Sun, J. Wu, F. Du, X. Chen, Z. J. Chen, *Science* **339**, 786–791 (2013).
3. J. Wu *et al.*, *Science* **339**, 826–830 (2013).
4. A. Ablasser *et al.*, *Nature* **498**, 380–384 (2013).
5. E. J. Diner *et al.*, *Cell Rep* **3**, 1355–1361 (2013).
6. P. Gao *et al.*, *Cell* **153**, 1094–1107 (2013).
7. X. Zhang *et al.*, *Mol. Cell* **51**, 226–235 (2013).
8. H. Ishikawa, G. N. Barber, *Cell. Mol. Life Sci.* **68**, 1157–1165 (2011).
9. *cGas*$^{-/-}$ mice were generated by in vitro fertilization using sperm harboring a targeted insertion at the *cGas/Mb21d1* locus. For details, see materials and methods in the supplementary materials.
10. J. D. Sauer *et al.*, *Infect. Immun.* **79**, 688–694 (2011).
11. D. B. Stetson, R. Medzhitov, *Immunity* **24**, 93–103 (2006).
12. M. Yoneyama *et al.*, *Nat. Immunol.* **5**, 730–737 (2004).
13. A. Ablasser *et al.*, *Nat. Immunol.* **10**, 1065–1072 (2009).
14. Y. H. Chiu, J. B. Macmillan, Z. J. Chen, *Cell* **138**, 576–591 (2009).
15. L. A. Samaniego, L. Neiderhiser, N. A. DeLuca, *J. Virol.* **72**, 3307–3320 (1998).
16. G. T. Melroe, N. A. DeLuca, D. M. Knipe, *J. Virol.* **78**, 8411–8420 (2004).
17. O. Takeuchi, S. Akira, *Cell* **140**, 805–820 (2010).
18. H. Ishikawa, Z. Ma, G. N. Barber, *Nature* **461**, 788–792 (2009).
19. C. J. Desmet, K. J. Ishii, *Nat. Rev. Immunol.* **12**, 479–491 (2012).
20. Z. Zhang *et al.*, *Nat. Immunol.* **12**, 959–965 (2011).
21. L. Unterholzner *et al.*, *Nat. Immunol.* **11**, 997–1004 (2010).
22. W. Chen, R. Kuolee, H. Yan, *Vaccine* **28**, 3080–3085 (2010).

Acknowledgments: We thank R. Hammer and the transgenic core facility at University of Texas Southwestern Medical Center for performing in vitro fertilization, S. Murray for technical assistance in HSV1 infection in mice, and N. DeLuca and D. Knipe for providing HSV1 strains d109 and 7134, respectively. This work was supported by grants from NIH (AI-093967) and the Cancer Prevention and Research Institute of Texas (RP110430). H.W. was supported by an NIH postdoctoral training grant (5T32AI070116). Z.J.C. is an investigator of Howard Hughes Medical Institute. The University of Texas has filed a patent on using cGAMP and its derivatives as vaccine adjuvants (U.S. patents 61/829,251 and 61/739.072; pharmaceutical targeting of a mammalian cyclic di-nucleotide signaling pathway). Materials including the *cGas*$^{-/-}$ mice may be requested upon signing a materials transfer agreement. The data presented in this manuscript are tabulated in the main paper and the supplementary materials.

Supplementary Materials

www.sciencemag.org/content/341/6152/1390/suppl/DC1
Materials and Methods
Figs. S1 to S6
References (*23*–*25*)

31 July 2013; accepted 16 August 2013
Published online 29 August 2013;
10.1126/science.1244040

Constitutive μ-Opioid Receptor Activity Leads to Long-Term Endogenous Analgesia and Dependence

G. Corder,[1] S. Doolen,[1] R. R. Donahue,[1] M. K. Winter,[2] B. L. Jutras,[3] Y. He,[4] X. Hu,[4] J. S. Wieskopf,[5] J. S. Mogil,[5] D. R. Storm,[6] Z. J. Wang,[4] K. E. McCarson,[2] B. K. Taylor[1]*

Opioid receptor antagonists increase hyperalgesia in humans and animals, which indicates that endogenous activation of opioid receptors provides relief from acute pain; however, the mechanisms of long-term opioid inhibition of pathological pain have remained elusive. We found that tissue injury produced μ-opioid receptor (MOR) constitutive activity (MOR_{CA}) that repressed spinal nociceptive signaling for months. Pharmacological blockade during the posthyperalgesia state with MOR inverse agonists reinstated central pain sensitization and precipitated hallmarks of opioid withdrawal (including adenosine 3′,5′-monophosphate overshoot and hyperalgesia) that required *N*-methyl-D-aspartate receptor activation of adenylyl cyclase type 1. Thus, MOR_{CA} initiates both analgesic signaling and a compensatory opponent process that generates endogenous opioid dependence. Tonic MOR_{CA} suppression of withdrawal hyperalgesia may prevent the transition from acute to chronic pain.

Chronic pain is determined by facilitatory mechanisms such as long-term potentiation (LTP) of synaptic strength in dorsal horn neurons (*1*–*3*). Whereas exogenously applied opiates prevent (*4*, *5*) and/or erase (*6*) spinal LTP, and spinal enkephalin release exerts inhibitory control of acute pain intensity soon after tissue injury (*7*, *8*), it remains unclear how the endogenous opioid system might persistently repress pathological pain. Opiates provide powerful pain relief, but repeated administration leads to the development of compensatory neuroadaptations underlying opiate tolerance and dependence (*9*), including the selective up-regulation of calcium-sensitive adenylyl cyclase (AC) isoforms (*10*, *11*). Cessation of opiates leads to cellular and behavioral symptoms of withdrawal (*12*–*16*). An intriguing hypothesis of drug addiction suggests that chronic opiates increase μ-opioid receptor (MOR) constitutive activity (MOR_{CA}) to preserve physical and psychological dependence (*17*–*21*), which is enhanced by enkephalins (*22*). Whether MORs adopt constitutive signaling states in other disease syndromes, such as chronic pain, is unknown. We tested the hypothesis that tissue injury increases MOR_{CA} in the spinal cord. With sufficient time after injury, enhanced basal MOR signaling should produce endogenous cellular and physical dependence in the CNS.

We first discovered that spinal opioid signaling promotes the intrinsic recovery of acute inflammatory pain and orchestrates long-lasting antinociception. In mice, a unilateral intraplantar injection of complete Freund's adjuvant (CFA) produced mechanical hyperalgesia that resolved within 10 days (Fig. 1A). Subcutaneous chronic minipump infusion of naltrexone hydrochloride (NTX), a nonselective opioid receptor antagonist, prolonged hyperalgesia throughout the 14-day infusion period in CFA-injured mice ($F_{3,17} = 25.4$, $P < 0.0001$) (Fig. 1B), although it had no effect in sham-injured mice. When the NTX pump was removed, hyperalgesia rapidly declined. NTX did not alter the induction phase of CFA-induced hyperalgesia (fig. S1, A and B, and supplementary text S1); however, when delivered 21 days after CFA injection (CFA-21d mice) in the complete absence of pain, systemic NTX reinstated hyperalgesia ($F_{1,21} = 41$, $P < 0.0001$) (Fig. 1C) in a dose-dependent manner with no effect in sham-injured mice (Fig. 1D). By contrast, systemic injection of naltrexone methobromide (NMB), an opioid receptor antagonist that does not cross the blood-brain barrier, failed to alter mechanical thresholds at either the ipsilateral or contralateral paws (both $P > 0.05$) (Fig. 1E). Intrathecal administration of either NTX or NMB precipitated robust hyperalgesia in CFA-treated mice after 21 days at both the injured ipsilateral paw ($P < 0.05$) (Fig. 1F) and uninjured contralateral paw ($P < 0.05$) (Fig. 1F), with no effect in sham-injured mice (Fig. 1G). NTX also induced heat hyperalgesia ($P < 0.05$) (Fig. 1H), as well as spontaneous pain in males ($P < 0.05$) (Fig. 1I) and females (fig. S3). Intrathecal NTX reinstated hyperalgesia in a model of postsurgical pain ($P < 0.05$)

[1]Department of Physiology, University of Kentucky, Lexington, KY 40536, USA. [2]Department of Pharmacology, Toxicology and Therapeutics, University of Kansas Medical Center, Kansas City, KS 66160, USA. [3]Department of Microbiology, Immunology and Molecular Genetics, University of Kentucky, Lexington, KY 40536, USA. [4]Department of Biopharmaceutical Sciences, University of Illinois, Chicago, IL 60612, USA. [5]Department of Psychology and Alan Edwards Centre for Research on Pain, McGill University, Montreal, Quebec H3A 1B1, Canada. [6]Department of Pharmacology, School of Medicine, University of Washington, Seattle, WA 98195, USA.

*Corresponding author. E-mail: brad.taylor@uky.edu

(Fig. 1J) (*23*), in several other models of inflammatory and neuropathic pain, and in multiple mouse strains.

Whether signaling with MOR and heterotrimeric GTP-binding protein (G protein) can be maintained for sufficient duration to oppose chronic pain is unknown. First, we found that disruption of $G\alpha_{i/o}$ signaling with intrathecal injection of pertussis toxin precipitated hyperalgesia in CFA-21d mice but not sham-injured mice ($P < 0.05$) (Fig. 1K). Second, we assessed guanosine-5′-*O*-(3-[^{35}S]thio)triphosphate ([^{35}S]GTP-γ-S) binding in fresh spinal cord slices (Fig. 1, L and M). In control slices, the MOR-selective agonist [D-Ala^2, *N*-methyl-Phe^4, Gly-ol^5]-enkephalin (DAMGO) elicited a stimulation of [^{35}S]GTP-γ-S binding with a maximum physiological effect (E_{max}) and median effective concentration (EC_{50}) of 58.02 ± 0.67% and 0.24 ± 0.01 μM, respectively (Fig. 1M). E_{max} was potentiated in CFA-21d slices not only in the ipsilateral dorsal horns (79.85 ± 7.35%, $P < 0.05$ compared with sham-injured) (Fig. 1M) but also in the contralateral dorsal horns (74.05 ± 4.13%, $P < 0.05$ compared with sham-injured)

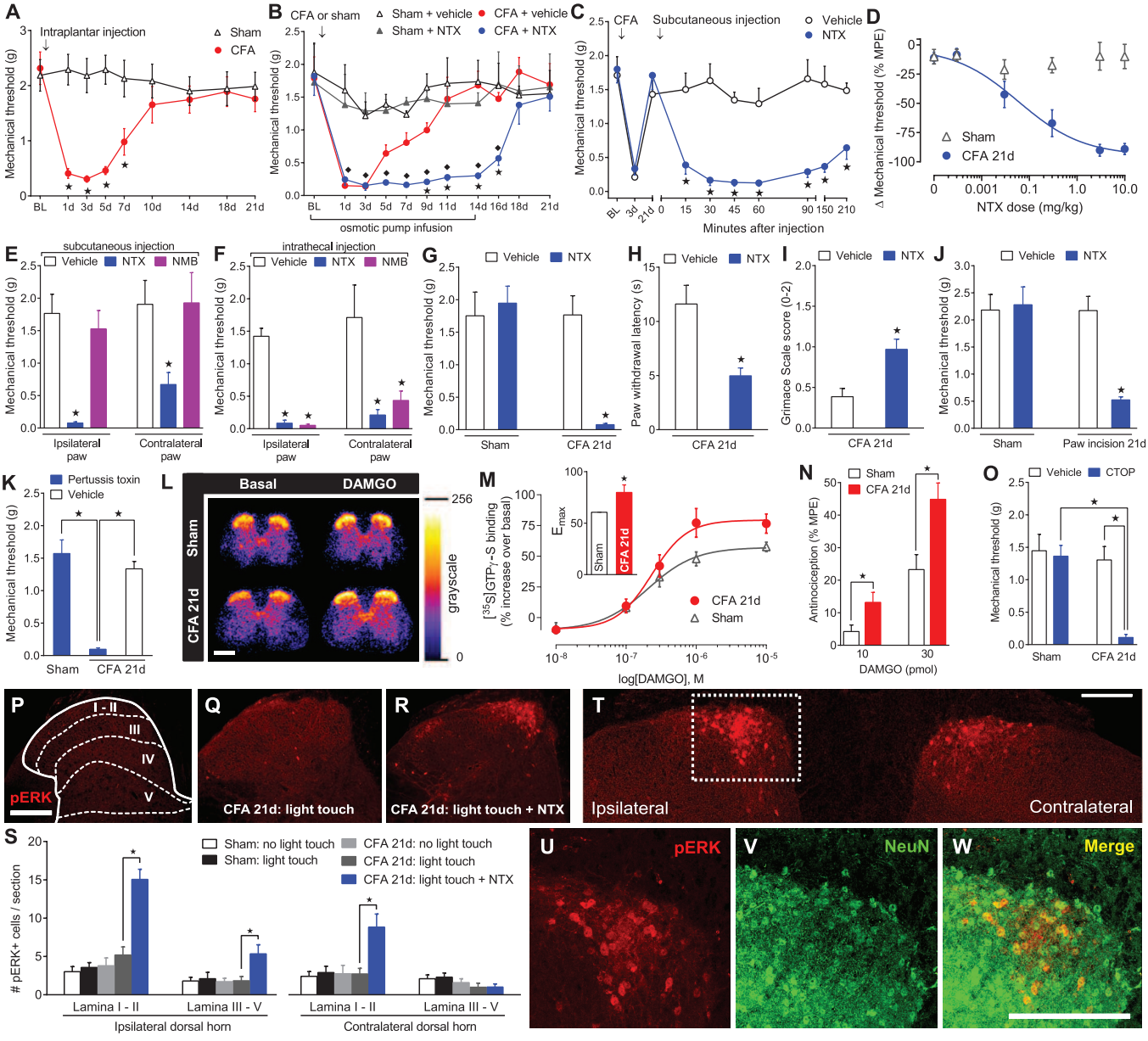

Fig. 1. Injury-induced pain sensitization is tonically opposed by spinal MOR–G-protein signaling. (**A**) Progression of mechanical hyperalgesia after intraplantar CFA (5 μl) injection ($n = 10$). (**B**) Resolution of hyperalgesia during and 14 days after infusion of NTX (10 mg/kg of body weight per day, subcutaneously) in sham-injured and CFA-injected mice ($n = 5$ to 6). ★$P <$ 0.05 compared with CFA+saline, ◆$P < 0.05$ compared with Sham+NTX. (**C**) Time course of reinstatement of hyperalgesia after subcutaneous NTX (3 mg/kg) in CFA-21d mice ($n = 6$ to 13). (**D**) Dose-response effects of NTX on hyperalgesia ($n = 6$ per dose). MPE: maximal possible effect. (**E** and **F**) Effect on hyperalgesia of (E) subcutaneous or (F) intrathecal NTX (3 mg/kg or 1 μg) or NMB (3 mg/kg or 0.3 μg) ($n = 5$ to 10). (**G** to **J**) Effect of intrathecal NTX (1 μg) on reinstatement of (G) mechanical hyperalgesia in sham-injured and CFA-injected mice ($n = 5$ to 8), (H) heat hyperalgesia ($n = 5$ to 10), (I) spontaneous pain ($n = 4$ to 8), and (J) postoperative pain ($n = 6$ to 11). (**K**) Effect of intrathecal pertussis toxin (0.5 μg) on hyperalgesia ($n = 6$). (**L**) Representative radiograms and (**M**) dose-response effects of DAMGO-stimulated [^{35}S]GTP-γ-S binding in lumbar spinal cord; (inset) binding E_{max} ($n = 7$ to 9). (**N**) Effect of DAMGO administered intrathecally on hotplate latency ($n = 8$). (**O**) Effect of intrathecal CTOP (100 ng) on hyperalgesia ($n = 6$ to 7). (**P** to **R**) Representative images and (**S**) dorsal horn laminar quantification (I and II and III to V) of light touch-evoked pERK after intrathecal NTX (1 μg) ($n = 5$ to 7). (**T**) Confocal image of pERK+ cells. (**U** to **W**) From boxed region in (T): Co-localization of pERK with the biomarker NeuN. All scale bars, 200 μm. ★$P < 0.05$ for all panels. All data shown as means ± SEM. See fig. S1 for full time-course data for (E) to (J) and (O).

(fig. S4), with no change in the EC_{50}. Third, the antinociceptive effects of intrathecal DAMGO were potentiated in CFA-21d mice ($P < 0.05$) (Fig. 1N), which reflected increases in receptor number, receptor affinity, or descending modulatory circuits. Fourth, intrathecal injection of Phe-Cys-Tyr-Trp-Orn-Thr-Pen-Thr-NH_2 (CTOP), a MOR-selective antagonist, reinstated hyperalgesia in CFA-21d mice but not sham-injured mice ($P < 0.05$) (Fig. 1M).

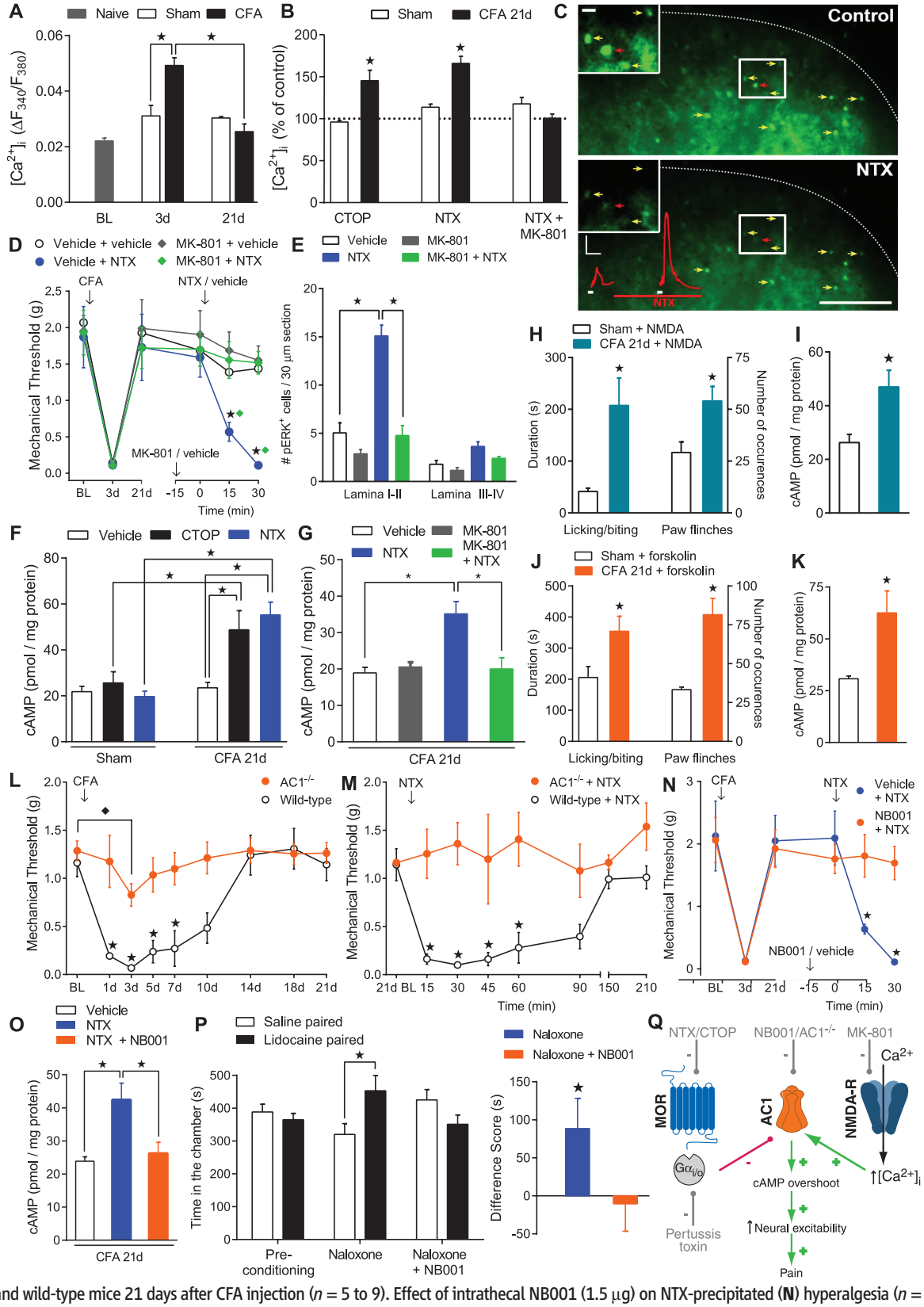

Fig. 2. Pain reinstatement requires potentiated NMDAR activation of calcium-sensitive AC 1. (**A**) Time course of glutamate-evoked (0.3 mM) $[Ca^{2+}]_i$ in spinal cord slices from sham-injured and CFA-injected mice ($n = 4$ to 7 mice) shown as the ratio of change in fluorescence intensity at 340 nm and 380 nm ($\Delta F_{340}/F_{380}$). Naïve BL, baseline. (**B**) Effect of CTOP (1 μM), NTX (10 μM), or NTX+MK-801 (100 μM) on $[Ca^{2+}]_i$. Values are relative to predrug control responses ($n = 3$ to 5 mice). (**C**) Representative fluorescence intensity at 380 nm, image of dorsal horn neurons from a CFA-21d slice responding to glutamate before (top) and after NTX (10 μM) (bottom) (yellow arrows). Decrease in fluorescence intensity corresponds to increase in $[Ca^{2+}]_i$. The red traces illustrate the rise in $[Ca^{2+}]_i$ for the indicated cell (red arrow). (Insets) Areas in white boxes. Scale bars: 0.02 for $\Delta F/F$ (vertical) and 3 min (horizontal), and 100 μm and 10 μm (inset). Effect of intrathecal MK-801 (1 μg) on NTX-precipitated (1 μg) (**D**) hyperalgesia and (**E**) touch-evoked dorsal horn pERK expression ($n = 5$ to 10). (**F**) Spinal cord cAMP levels after intrathecal vehicle ($n = 14$ to 18), CTOP (100 ng; $n = 6$), or NTX (1 μg; $n = 6$ to 10). (**G**) Effect of intrathecal MK-801 (1 μg) on NTX-precipitated spinal cAMP overshoot ($n = 5$). (**H** to **K**) Effect of intrathecal NMDA (3 pmol; $n = 5$ to 7) or forskolin (1.5 μg; $n = 6$) on (H and J) spontaneous nocifensive behaviors and (I and K) spinal cAMP levels. (**L**) Progression of mechanical hyperalgesia and (**M**) effect of intrathecal NTX in $AC1^{-/-}$ and wild-type mice 21 days after CFA injection ($n = 5$ to 9). Effect of intrathecal NB001 (1.5 μg) on NTX-precipitated (**N**) hyperalgesia ($n = 4$ to 7), (**O**) spinal cAMP levels ($n = 6$ to 9), and (**P**) affective pain ($n = 6$ to 12). (**Q**) Schematic of cellular pathways involved in endogenous opioid withdrawal and pain reinstatement. ★, ◆, *$P < 0.05$.

We next asked whether central sensitization (increased responsiveness of CNS nociceptive neurons to normal or subthreshold afferent input) silently persists in the posthyperalgesia state under the control of endogenous MOR inhibition. Tested 21 days after CFA injection, an innocuous light touching of the injured hindpaw did not increase the dorsal horn expression of phosphorylated extracellular signal–regulated kinase (pERK) (Fig. 1, Q and S). However, intrathecal NTX increased touch-evoked pERK in lamina I and II ($P < 0.05$) (Fig. 1, R and S, and fig. S4) and III to V ($P < 0.05$) (Fig. 1, R and S). NTX also increased pERK at the contralateral dorsal horn (opiates $P < 0.05$) (Fig. 1, S and T). Confocal microscopy revealed that pERK was expressed in neurons (Fig. 1, U to W, and fig. S5) but not in microglia or astrocytes (fig. S5).

We next tested the hypothesis that *N*-methyl-D-aspartate receptor (NMDAR)–Ca^{2+}-dependent mechanisms of central sensitization (*1*, *24*) continue to operate after the resolution of inflammatory pain. Using live-cell Fura-2 ratiometric analysis in adult spinal cord slices (*25*), we found that glutamate-evoked intracellular calcium (Ca^{2+}) in lamina II neurons was potentiated 3 days after CFA injection and then resolved by day 21 ($F_{3,17} = 15$, $P < 0.0001$) (Fig. 2A). This potentiation coincides with the temporal onset and resolution of inflammatory hyperalgesia. Perfusion of either CTOP or NTX increased the peak amplitude of glutamate-evoked intracellular Ca^{2+} in CFA-21d slices but not sham-injured slices [lamina II: $P < 0.05$

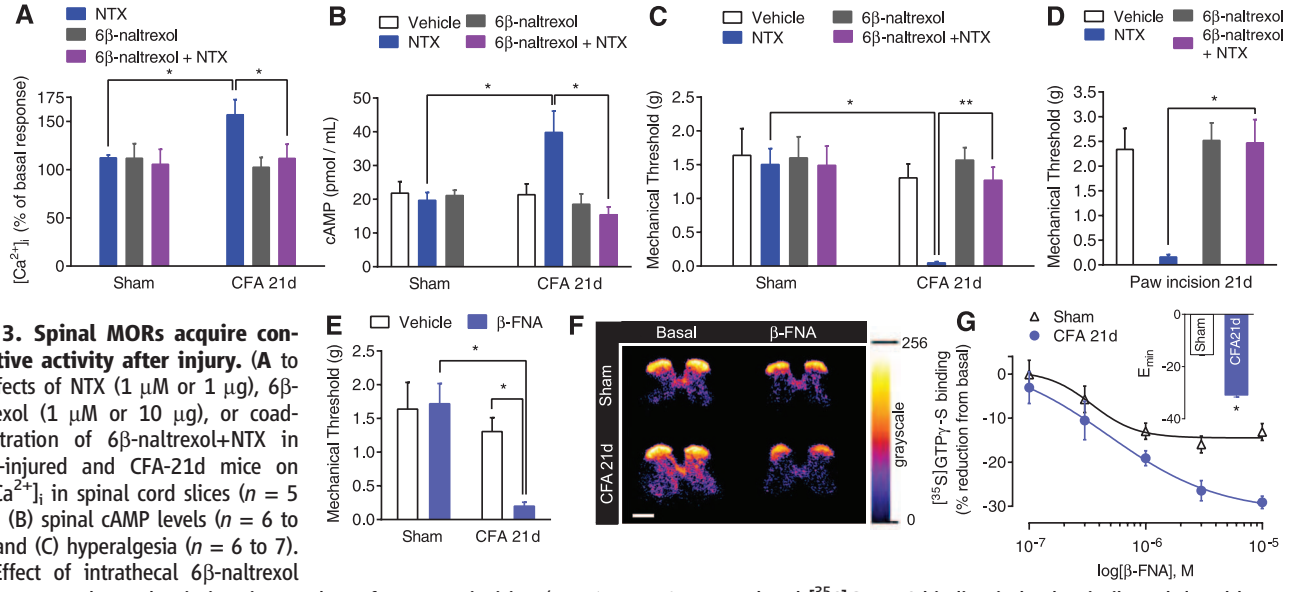

Fig. 3. Spinal MORs acquire constitutive activity after injury. (**A** to **C**) Effects of NTX (1 μM or 1 μg), 6β-naltrexol (1 μM or 10 μg), or coadministration of 6β-naltrexol+NTX in sham-injured and CFA-21d mice on (A) $[Ca^{2+}]_i$ in spinal cord slices (n = 5 to 6), (B) spinal cAMP levels (n = 6 to 11), and (C) hyperalgesia (n = 6 to 7). (**D**) Effect of intrathecal 6β-naltrexol and/or NTX on hyperalgesia in mice 21 days after a paw incision (n = 6 to 7). (**E**) Effect of intrathecal β-funaltrexamine (β-FNA, 2.5 μg) on hyperalgesia (n = 6 to 7). (**F**) Representative radiograms and (**G**) dose-response effects of β-FNA on basal [^{35}S]GTP-γ-S binding in lumbar ipsilateral dorsal horn; (inset) binding E_{max} (n = 7 to 9). *$P < 0.05$. All data are shown as means ± SEM. See fig. S9 for full time-course data of (C) to (E).

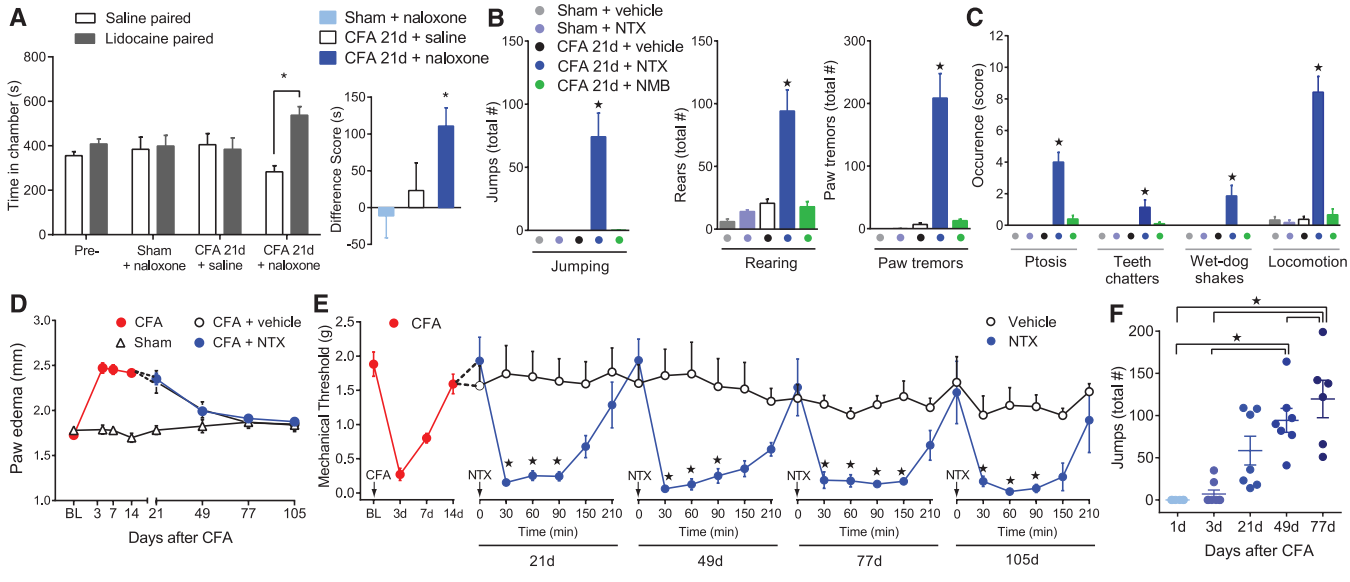

Fig. 4. Prolonged endogenous MOR signaling generates psychological and physical dependence. (**A**) Behavioral signs of psychological withdrawal (aversion associated with spontaneous pain) were reflected by place preference for intrathecal lidocaine upon naloxone administration. (Left) Intragroup chamber analysis for intrathecal saline (5 μl) or lidocaine (0.04%) in sham-injured and CFA-21d mice treated with intraperitoneal saline or naloxone (3 mg/kg). (Right) Intergroup difference score analysis illustrating time spent in intrathecal lidocaine-paired chambers (n = 6 per group). (**B** and **C**) Behavioral signs of physical withdrawal, recorded for 60 min after injection of NTX (3 mg/kg), NMB (3 mg/kg), or vehicle (n = 6 to 7). (**D**) Progression of paw edema and (**E**) effects of repeated subcutaneous vehicle or NTX (3 mg/kg) on hyperalgesia over 105 days after CFA (n = 7 per group). (**F**) Effect of repeated NTX (3 mg/kg) on the number of precipitated escape jumps over 77 days after CFA (n = 8). *, ★$P < 0.05$. All data shown as means ± SEM.

(Fig. 2, B and C, and fig. S6); lamina I: $P < 0.05$ (fig. S7)] or CFA-injured slices after 24 hours (fig. S1C). The activity-dependent NMDAR blocker, MK-801, prevented the NTX-mediated rise in intracellular calcium concentration $[Ca^{2+}]_i$ ($F_{1,16} = 4.6$, $P < 0.05$) (Fig. 2C), hyperalgesia ($F_{3,22} = 6.5$, $P < 0.005$) (Fig. 2D) and dorsal horn pERK levels ($P < 0.05$) (Fig. 2E, ipsilateral and fig. S8, contralateral).

Opioids produce their acute actions in part through inhibition of ACs, whereas chronic opiate exposure produces a homeostatic up-regulation of ACs (*9*, *14*). In this opioid-dependent state, receptor antagonists produce cellular withdrawal, characterized by an adenosine 3′,5′-cyclic monophosphate (cAMP) overshoot response. To determine whether similar homeostatic mechanisms operate in the setting of tonic opioid receptor signaling after injury, we sampled intracellular cAMP content from ex vivo lumbar spinal tissue. Basal spinal cAMP levels were comparable in sham-injured and CFA-21d mice, suggestive of a return to baseline AC function (Fig. 2F and supplementary text S2). In CFA-21d mice, however, intrathecal CTOP or NTX increased cAMP levels in CFA-21d mice ($P < 0.05$) (Fig. 2F), indicative of AC superactivation. Because the Ca^{2+}-stimulated isoforms of ACs are activated by NMDARs (*26*), we hypothesized that NMDAR signaling contributes to this cAMP overshoot. Intrathecal MK-801 abolished the NTX-precipitated increases in cAMP ($P < 0.05$ compared with NTX group) (Fig. 2G). Moreover, direct activation of spinal NMDARs and ACs by intrathecal NMDA or forskolin, respectively, increased nocifensive behaviors ($P < 0.05$) (Fig. 2, H and J) and spinal cAMP levels ($P < 0.05$) (Fig. 2, I and K) in CFA-21d mice as compared with sham-injured mice, which suggests latent up-regulation, but not occlusion, of NMDAR–AC pathways.

Adenylyl cyclase type 1 (AC1) in the brain is intricately linked to morphine dependence (*27*, *28*) and chronic pain (*29*), whereas in the spinal cord, it contributes to activity-dependent LTP (*30*). Baseline mechanical thresholds were similar in wild-type and AC1 knockout mice ($AC1^{-/-}$) (*29*) (Fig. 2L). However, AC1 gene deletion reduced inflammatory hyperalgesia (3 days later versus baseline: $P < 0.05$, *t* test; $F_{1,11} = 31.5$, $P < 0.0005$, Genotype × Time) (Fig. 2L), without affecting edema (fig. S9). At day 21 after CFA treatment, NTX reinstatement was lost in $AC1^{-/-}$ mice ($F_{1,7} = 20.3$, $P < 0.005$) (Fig. 2M). Furthermore, intrathecal NB001, a selective AC1 inhibitor (*30*), prevented NTX-based reinstatement of hyperalgesia ($F_{1,9} = 6.6$, $P < 0.05$) (Fig. 2N), as well as cAMP overshoot and spontaneous pain ($P < 0.05$) (Fig. 2, O and P). These data suggest that withdrawal from tonic MOR signaling increases pronociceptive neural excitability consequent to AC1 superactivation (Fig. 2Q).

Tonic MOR signaling arises from either continuous agonist stimulation or constitutive (agonist-independent) activity (*31*–*34*). MOR_{CA} develops with chronic morphine administration and leads to physical and affective signs of opiate dependence and addiction (*17*, *19*–*22*). To determine the existence and physiologic significance of MOR_{CA} in pathological pain processing, we used the neutral antagonist 6β-naltrexol, a structural analog of NTX (*35*). Intrathecal 6β-naltrexol alone did not change Ca^{2+} levels in sham-injured or CFA-21d spinal slices (Fig. 3A) and failed to precipitate a cAMP overshoot (Fig. 3B) or hyperalgesia (Fig. 3C). 6β-Naltrexol abolished the ability of NTX to produce Ca^{2+} mobilization ($P < 0.05$) (Fig. 3A), cAMP overshoot ($P < 0.05$) (Fig. 3B), and hyperalgesia in CFA-21d mice ($P < 0.05$) (Fig. 3C). 6β-Naltrexol also abolished NTX-induced reinstatement of mechanical hyperalgesia in a postoperative pain model (*23*) (Fig. 3D). These data suggest that NTX acts as an inverse agonist to inactivate MOR_{CA} in multiple models of inflammatory pain (supplementary text S3 and S4) (*36*, *37*).

Intrathecal administration of an alternative μ-selective inverse agonist, β-funaltrexamine (β-FNA) (*38*), reinstated hyperalgesia in CFA-21d, but not sham-injured, mice ($P < 0.05$) (Fig. 3E). Because MOR_{CA} results in elevated basal G protein cycling (*19*, *38*), we determined whether β-FNA could promote the MOR-inactive state and, thereby, decrease spontaneous basal GDP/GTP-γ-S exchange. β-FNA reduced basal [^{35}S]GTP-γ-S binding in a concentration-dependent manner in dorsal horn sections from CFA-21d mice and, to a significantly lesser degree, sham-injured mice, in both ipsilateral and contralateral dorsal horns (Fig. 3, F and G, and fig. S11).

Pain comprises sensory (hyperalgesia) and affective (aversiveness) components; the latter can be identified by changes in the rewarding property of analgesics and associated motivational behavior. In a conditioned place preference paradigm (*39*–*41*), the negative reinforcing capacity of intrathecal lidocaine (motivation to seek pain relief) demonstrates the presence of aversive pain 1 day after CFA injection (*40*). This aversive component was absent at 21 days (Fig. 4A, CFA-21d+saline group). CFA-21d, but not sham-injured, mice responded to systemic naloxone by spending more time in the chamber paired with intrathecal lidocaine (538 ± 39 s) than with intrathecal saline (283 ± 28 s, $P < 0.001$) (Fig. 4A). Systemic NTX, but not saline or NMB, precipitated numerous escape and somato-motor behaviors analogous to classical morphine withdrawal (*42*, *43*) in CFA-21d mice, with no effect in sham-injured mice (Fig. 4, B and C).

To determine whether pain sensitization and endogenous opioid physical dependence persist beyond tissue healing, we gave periodic injections of NTX during and after the course of inflammatory edema, which subsided within 77 days after CFA injection (Fig. 4D). NTX, but not saline, reinstated hyperalgesia for at least 105 days after CFA treatment (21 days: $F_{1,80} = 8.5$, $P < 0.05$; 49 days: $F_{1,72} = 59$, $P < 0.0001$; 77 days: $F_{1,72} = 76$, $P < 0.0001$; 105 days: $F_{1,64} = 33$, $P < 0.0001$) (Fig. 4E). This was true 200 days after CFA injection (fig. S12 and supplementary text S5), and after a single intrathecal injection 105 days after CFA injection, without prior exposure of the animal to the testing environment, of NTX or CTOP (fig. S12). NTX-precipitated escape-jump frequency increased with time after the injury ($F_{4,29} = 14$, $P < 0.0001$) (Fig. 4F), which suggested that intensifying opioidergic and compensatory neuroadaptations create a physical and psychological dependence that greatly outlasts acute pain and tissue injury (supplementary text S6).

These data indicate that blockade of MOR_{CA} unmasks a silent AC1 central sensitization pathway that persists beyond the resolution of pain and inflammation, reflective of hyperalgesic priming (*44*). The presence of contralateral spinal MOR_{CA} and neural sensitization illustrates the spread of this pathology to areas of the CNS beyond those directly innervated by the injured tissue. Thus, MOR_{CA} might tonically repress widespread hyperalgesia (supplementary text S7). If true, then loss of MOR_{CA} antinociception (e.g., during stress) could lead to the emergence of rampant chronic pain (*45*, *46*).

We have identified an injury-induced MOR_{CA} that promotes both endogenous analgesia and dependence. Our data suggest that long-term MOR_{CA} inhibition of AC1-mediated central sensitization drives a counteradaptive, homeostatic increase in pronociceptive AC1 signaling cascades (*29*, *47*) and thereby paradoxically promotes the maintenance of latent central sensitization. Thus, injury produces a long-lasting dependence on MOR_{CA} that tonically prevents withdrawal hyperalgesia, consistent with proposed mechanisms of dependence to opiate drugs such as morphine (*27*, *48*). We contend that loss of MOR_{CA}, and the ensuing reinstatement of pain, reflects a process of spinal cellular withdrawal (NMDA-mediated AC1 superactivation) to enhance pronociceptive synaptic strength (supplementary text S8) (*49*, *50*), as observed after NMDA-R–dependent spinal LTP at C-fiber synapses during withdrawal from exogenous opiates (*12*). Indeed, stress (*46*) or injury (*51*) escalates opposing inhibitory and excitatory influences on nociceptive processing, as a pathological consequence of increased endogenous opioid tone. This raises the prospect that opposing homeostatic interactions between MOR_{CA} analgesia and latent NMDA-R–AC1 pain sensitization create a lasting susceptibility to develop chronic pain.

References and Notes

1. A. Latremoliere, C. J. Woolf, *J. Pain* **10**, 895–926 (2009).
2. H. Ikeda *et al.*, *Science* **312**, 1659–1662 (2006).
3. R. Ruscheweyh, O. Wilder-Smith, R. Drdla, X. G. Liu, J. Sandkühler, *Mol. Pain* **7**, 20 (2011).
4. G. W. Terman, C. L. Eastman, C. Chavkin, *J. Neurophysiol.* **85**, 485–494 (2001).
5. J. Benrath, C. Brechtel, E. Martin, J. Sandkühler, *Anesthesiology* **100**, 1545–1551 (2004).
6. R. Drdla-Schutting, J. Benrath, G. Wunderbaldinger, J. Sandkühler, *Science* **335**, 235–238 (2012).
7. A. I. Basbaum, H. L. Fields, *Annu. Rev. Neurosci.* **7**, 309–338 (1984).
8. M. H. Ossipov, G. O. Dussor, F. Porreca, *J. Clin. Invest.* **120**, 3779–3787 (2010).
9. M. J. Christie, *Br. J. Pharmacol.* **154**, 384–396 (2008).
10. T. Avidor-Reiss, I. Nevo, D. Saya, M. Bayewitch, Z. Vogel, *J. Biol. Chem.* **272**, 5040–5047 (1997).

11. S. B. Lane-Ladd *et al.*, *J. Neurosci.* **17**, 7890–7901 (1997).
12. R. Drdla, M. Gassner, E. Gingl, J. Sandkühler, *Science* **325**, 207–210 (2009).
13. C. Heinl, R. Drdla-Schutting, D. N. Xanthos, J. Sandkühler, *J. Neurosci.* **31**, 16748–16756 (2011).
14. E. J. Nestler, G. K. Aghajanian, *Science* **278**, 58–63 (1997).
15. J. A. Kauer, R. C. Malenka, *Nat. Rev. Neurosci.* **8**, 844–858 (2007).
16. M. S. Angst, J. D. Clark, *Anesthesiology* **104**, 570–587 (2006).
17. Z. Wang, E. J. Bilsky, F. Porreca, W. Sadée, *Life Sci.* **54**, PL339–PL350 (1994).
18. J. G. Liu, P. L. Prather, *Mol. Pharmacol.* **60**, 53–62 (2001).
19. D. Wang *et al.*, *J. Pharmacol. Exp. Ther.* **308**, 512–520 (2004).
20. J. R. Shoblock, N. T. Maidment, *Neuropsychopharmacology* **31**, 171–177 (2006).
21. F. J. Meye, R. van Zessen, M. P. Smidt, R. A. Adan, G. M. Ramakers, *J. Neurosci.* **32**, 16120–16128 (2012).
22. J. R. Shoblock, N. T. Maidment, *Neuroscience* **149**, 642–649 (2007).
23. E. M. Pogatzki, S. N. Raja, *Anesthesiology* **99**, 1023–1027 (2003).
24. C. Luo, P. H. Seeburg, R. Sprengel, R. Kuner, *Pain* **140**, 358–367 (2008).
25. S. Doolen, C. B. Blake, B. N. Smith, B. K. Taylor, *Mol. Pain* **8**, 56 (2012).
26. D. M. Chetkovich, J. D. Sweatt, *J. Neurochem.* **61**, 1933–1942 (1993).
27. V. Zachariou *et al.*, *Biol. Psychiatry* **63**, 1013–1021 (2008).
28. M. S. Mazei-Robison, E. J. Nestler, *Cold Spring Harbor Perspect. Med.* **2**, a012070 (2012).
29. F. Wei *et al.*, *Neuron* **36**, 713–726 (2002).
30. H. Wang *et al.*, *Sci. Transl. Med.* **3**, 65ra3 (2011).
31. T. Kenakin, *FASEB J.* **15**, 598–611 (2001).
32. T. Kenakin, *Trends Pharmacol. Sci.* **25**, 186–192 (2004).
33. T. Costa, A. Herz, *Proc. Natl. Acad. Sci. U.S.A.* **86**, 7321–7325 (1989).
34. R. Seifert, K. Wenzel-Seifert, *Naunyn Schmiedebergs Arch. Pharmacol.* **366**, 381–416 (2002).
35. K. M. Raehal *et al.*, *J. Pharmacol. Exp. Ther.* **313**, 1150–1162 (2005).
36. W. Sadée, D. Wang, E. J. Bilsky, *Life Sci.* **76**, 1427–1437 (2005).
37. H. Lam *et al.*, *Mol. Pain* **7**, 24 (2011).
38. J. G. Liu, M. B. Ruckle, P. L. Prather, *J. Biol. Chem.* **276**, 37779–37786 (2001).
39. T. King *et al.*, *Nat. Neurosci.* **12**, 1364–1366 (2009).
40. Y. He, X. Tian, X. Hu, F. Porreca, Z. J. Wang, *J. Pain* **13**, 598–607 (2012).
41. K. J. Sufka, *Pain* **58**, 355–366 (1994).
42. G. F. Koob, R. Maldonado, L. Stinus, *Trends Neurosci.* **15**, 186–191 (1992).
43. B. Kest *et al.*, *Neuroscience* **115**, 463–469 (2002).
44. M. N. Asiedu *et al.*, *J. Neurosci.* **31**, 6646–6653 (2011).
45. M. De Felice *et al.*, *Brain* **133**, 2475–2488 (2010).
46. C. Rivat *et al.*, *Neuropsychopharmacology* **32**, 2217–2228 (2007).
47. M. Zhuo, *Drug Discov. Today* **17**, 573–582 (2012).
48. S. Li *et al.*, *Mol. Pharmacol.* **70**, 1742–1749 (2006).
49. H. C. Lu *et al.*, *Nat. Neurosci.* **6**, 939–947 (2003).
50. H. Xu *et al.*, *J. Neurosci.* **28**, 7445–7453 (2008).
51. C. Rivat *et al.*, *Anesthesiology* **96**, 381–391 (2002).

Acknowledgments: The authors thank H. L. Fields, A. I. Basbaum, L. Hough, J. C. Marvizon, E. Bilsky, W. Sadee, G. Scherrer, K. Westlund High, M. Werner, J. Dahl, and B. Solway for critical discussions and J. Grasch, L. Martin, and R. Griggs for technical assistance and blinding. This work was supported by NIH grants F31DA032496 (G.C.), HD02528 (M.K.W. and K.E.M.), R01NS45954 (B.K.T.), and 5K02DA19656 (B.K.T.). Author contributions: G.C. and B.K.T. formulated the hypotheses, designed, analyzed and coordinated all experiments. G.C. performed surgeries, behavioral pharmacology, histology, and fluorescence imaging and analyzed the data. G.C. and B.L.J. carried out the biochemical studies and G.C. analyzed the data. S.D. and G.C. carried out Ca^{2+} imagining experiments and analyzed the data. M.K.W., K.E.M., G.C., and B.K.T. designed the [^{35}S]GTP-γ-S binding studies; M.K.W. collected the data; and G.C., K.E.M., and B.K.T. analyzed the data. D.R.S. supplied the $AC1^{-/-}$ breeders. Z.J.W., G.C., and B.K.T. designed the conditioned place preference experiments, and Y.H. and X.H. conducted experiments and analyzed the data. J.S.M., J.S.W., G.C., and B.K.T. designed the Mouse Grimace Scale experiments, and J.W. conducted the experiments. R.R.D. conducted the plantar incision studies. G.C. and B.K.T. wrote the manuscript.

Supplementary Materials

www.sciencemag.org/content/341/6152/1394/suppl/DC1
Materials and Methods
Supplementary Text
Figs. S1 to S13
References (*52*–*80*)

19 April 2013; accepted 20 August 2013
10.1126/science.1239403

Human LilrB2 Is a β-Amyloid Receptor and Its Murine Homolog PirB Regulates Synaptic Plasticity in an Alzheimer's Model

Taeho Kim,[1]* George S. Vidal,[1] Maja Djurisic,[1] Christopher M. William,[2] Michael E. Birnbaum,[3] K. Christopher Garcia,[3] Bradley T. Hyman,[2] Carla J. Shatz[1]*

Soluble β-amyloid (Aβ) oligomers impair synaptic plasticity and cause synaptic loss associated with Alzheimer's disease (AD). We report that murine PirB (paired immunoglobulin-like receptor B) and its human ortholog LilrB2 (leukocyte immunoglobulin-like receptor B2), present in human brain, are receptors for Aβ oligomers, with nanomolar affinity. The first two extracellular immunoglobulin (Ig) domains of PirB and LilrB2 mediate this interaction, leading to enhanced cofilin signaling, also seen in human AD brains. In mice, the deleterious effect of Aβ oligomers on hippocampal long-term potentiation required PirB, and in a transgenic model of AD, PirB not only contributed to memory deficits present in adult mice, but also mediated loss of synaptic plasticity in juvenile visual cortex. These findings imply that LilrB2 contributes to human AD neuropathology and suggest therapeutic uses of blocking LilrB2 function.

Soluble oligomeric species of β-amyloid (Aβ) are thought to be key mediators of cognitive dysfunction in Alzheimer's disease (AD) (*1*, *2*). Transgenic mice expressing elevated levels of human Aβ experience memory loss and synaptic regression (*3*–*6*). Aβ production is thought to be activity-dependent (*7*, *8*), and even in wild-type mice, addition of soluble Aβ oligomers to hippocampal slices or cultures induces loss of long-term potentiation (LTP), increases long-term depression (LTD), and decreases dendritic spine density (*9*–*11*). Aβ oligomers may exert some of their adverse effects on synaptic plasticity and memory by binding to receptors, thereby perturbing or engaging downstream signaling. At least two Aβ receptors, cellular prion protein (PrP^C) and ephrin type B receptor 2 (EphB2), have been identified, and downstream signaling from both alters *N*-methyl-D-aspartate (NMDA) receptor function in response to Aβ (*6*, *12*, *13*). Aβ oligomers are also known to engage other signaling pathways, including the actin-severing protein cofilin and protein phosphatases PP2A and PP2B/calcineurin, thereby mediating spine loss and synaptic defects (*9*, *14*); however, signaling upstream of these pathways is not well understood.

Recently, a very early loss of activity-dependent plasticity was discovered in vivo in APP/PS1 transgenic mice, an AD model in which mutant alleles of both amyloid precursor protein (APPswe) and presenilin 1 (PSEN1ΔE9) are expressed (*15*, *16*): Ocular dominance plasticity (ODP) during the critical period of development in visual cortex [postnatal day 22 (P22) to P32] is defective (*17*). This observation directly contrasts with mice lacking PirB (paired immunoglobulin-like receptor B), in which ODP is enhanced during the critical period and in adults (*18*). PirB, a receptor originally thought to function exclusively in the immune system (*19*), is now also known to be expressed by neurons, present in neuronal growth cones, and associated with synapses (*18*, *20*). Thus, it is possible that Aβ acts through PirB to diminish ODP in APP/PS1 mice.

To determine whether PirB can act as a receptor for soluble Aβ oligomers, we prepared biotinylated synthetic human $Aβ_{1-42}$ (Aβ42) peptides either without (mono-Aβ42) or with oligomerization (oligo-Aβ42; consists primarily of high-*n* oligomers) (Fig. 1, A and B, and fig. S1A) (*12*, *21*, *22*). We then measured binding of Aβ42 peptides to human embryonic kidney (HEK) 293 cells that expressed mouse PirB (PirB-IRES-EGFP) or control vector (IRES-EGFP). Relative to monomeric Aβ42, oligomerized Aβ42 peptides bound to PirB-expressing cells about 6 times as much (Fig. 1, A to D). Oligo-Aβ42 was consistently associated with PirB protein, as seen both by coimmunostaining (Fig. 1E, arrowheads) and by coimmunoprecipitation (fig. S1, B and C), indicating a direct interaction with PirB. This assay also confirms previously reported Nogo-66 binding to PirB (fig. S2) (*20*). In contrast, binding of Aβ42 oligomers was not evident in heterologous cells expressing mouse

[1]Departments of Biology and Neurobiology and Bio-X, James H. Clark Center, Stanford University, Stanford, CA 94305, USA. [2]Neuropathology Service, Massachusetts General Hospital, Charlestown, MA 02129, USA. [3]Howard Hughes Medical Institute, Department of Molecular and Cellular Physiology, and Department of Structural Biology, Stanford University School of Medicine, Stanford, CA 94305, USA.

*Corresponding author. E-mail: cshatz@stanford.edu (C.J.S.); tkim808@stanford.edu (T.K.)